IIUC Journal of Science and Engineering
Vol.-2, Issue-1, December 2024, pp. 105-120
ISSN: 3005-5873

Variations of axial and radial temperature inside the HLTP for microalgae cell growth

Md. Rashedul Islam
Department of Computer Science and Engineering
International Islamic University Chittagong (IIUC), Bangladesh

Article info

Keywords
Simulation
Microalgae
Photobioreactor
Biofuel
Axial
Radial Temperature

Abstract

The demand for microalgae-based biofuel has been attracted globally due to huge fuel demand and the global warming crisis. In this study, we simulated the axial and radial temperatures for microalgae cell growth. The computational domain is considered a horizontal loop tubular photobioreactor (HLTP) due to its high productivity. However, due to proper temperature variations, the growth is obtained as expected. We found that for proper cell growth, the standard temperature range is 293K–308K. From our simulation, we observed that the maximum temperature is near 312K through the axial direction and the maximum temperature is near 314K through the radial direction.

Corresponding author
Md. Rashedul Islam
Department of Computer Science and Engineering, International Islamic University Chittagong, Kumira, Chattogram, Bangladesh - 4318
Email: rashed_maths@yahoo.com

Introduction

The world has faced two major crises at the start of the twenty-first century: the first is the deterioration of fossil fuels as a consequence of increased use, and the second is the ensuing dependency on fossil fuel exporters in the world (Deb, Shahriar, Bhowmik & Chowdury, 2017*)*. In the recent world, the climate change, rising rising greenhouse gas (GHG) concentrations, depletion of the ozone layer, as well as other environmental problems arise from the burning of fossil fuels. The future of the fuel sector would be a disastrous if we are unable to generate suitable and cost-effective replacements for fossil fuels before they are depleted. To address this global energy demand, an efficient use of existing renewable natural resources is required. As the plant based bio-fuels is a potential renewable and carbon neutral alternative to the petroleum fuels (Smith, Sturm, Noyelles & Billings, 2010). Biofuel generation from crops is still more expensive than fossil fuels due to the

enormous quantity of arable land required (Khanam & Deb, 2016). Therefore, an alternative feedstock is necessary, to reduce worldwide demand and commercialize the manufacturing of biofuels. Researchers and engineers have been very interested in microalgae-based biofuel as a substitute feedstock for various other biofuel sources over the past few decades (Chisty, 2007). Microalgae can generate many kinds of biofuels, as like bioethanol, biodiesel, biohydrogen, biobutanol, bioelectricity and syngas (Chang et. al., 2017; Su, Song, Zhang, Su, Cheng & Chen, 2017).

Microalgae are cultivated mainly two systems; they are Open Raceway Ponds System and Closed Photobioreactors System (PBR) (Tredici, 1999). In case of PBR method, the growth of microalgae is affected by a combination of culture parameters. The fixed factors are geographical location, reactor geometry, and variable factors are light, temperature, wind speed, pH, CO_2, nutrients etc. Out of all these temperatures is a critical parameter because it has direct impact on the rate of microalgae growth. Microalgae culturing devices need to be optimized in terms of design and operation, temperature is a very important factor and it should be considered. Therefore, we should regulate the overall temperature to ensure that the cells reach its maximum potential.

The emission of light energy from the complete disk of the sun, evaluated at the Earth, is known as the solar irradiance. The associated temperature related to the solar irradiance in a tubular reactor has a significant impact on microalgae cell growth. Thus, using a mathematical computational growth model to estimate the effects of radial and axial temperature variations depending on the rate of growth and thermodynamic equilibrium for a horizontal loop tubular photobioreactor (HLTP), the related environmental data are taken from the geographical area of CUET, Chittagong, Bangladesh. Chlorella vulgaris was the microalgae strain which employed in our simulation.

Mathematical model

In our simulation, the algal suspension is treated as a compressible viscous single-phase Newtonian fluid, with single-phase laminar flow in the creeping condition as the flow issue. So the equation of continuity and the Navier-Stokes equations with coupled partial differential equations: the temperature balance equation and the algal cell concentration balance equation are the governing equations. As algal suspension is a Newtonian compressible fluid and the flow dynamics in our simulation are supposed to be laminar. Considering this perspective, the phenomenon of flow, fulfills the equation of continuity and the Navier Stokes equation that are given below:

$$\frac{\partial \rho}{\partial t} + \nabla.(\rho \boldsymbol{v}) = 0 \quad (1)$$

$$\rho \frac{\partial \boldsymbol{v}}{\partial t} + \rho \boldsymbol{v}.\nabla \boldsymbol{v} = -\nabla \rho + \nabla.\mu\left((\nabla \boldsymbol{v} + (\nabla \boldsymbol{v})^T) - \frac{2}{3}\mu(\nabla.\boldsymbol{v})\boldsymbol{I}\right) + \boldsymbol{F} \quad (2)$$

where, ρ represents the reactor medium's density (kgm^{-3}), $\boldsymbol{v}$ represents the velocity of the flow (ms^{-1}), μ represents the viscosity (kgm^{-1}s^{-1}) of the flow, $\boldsymbol{I}$ denotes the identity tensor, and $\boldsymbol{F}$ stands for the body force (N).

For a non-isothermal laminar flow, the heat transfer equation is

$$\rho C_p\left(\frac{\partial T}{\partial t} + \boldsymbol{v}.\nabla T\right) = \nabla.(k\nabla T) \quad (3)$$

where, C_p stands for the suspension's specific heat capacity (Jkg^{-1}K^{-1}), T represent the broth temperature (K) of the reactor and k stands for the thermal conductivity (Wm^{-1}K^{-1}).

In equation (2), the dynamic viscosity is expressed by the equation

$$\mu = \mu_0\{1 + \varepsilon C(t)\} \quad (4)$$

where, ε represents the coefficient Einstein (Einstein, 1906), μ_0 represents the viscosity (kgm^{-1}s^{-1}) of water and $C(t)$ stands for the concentration of microalgae at any given time t (g/L). According to findings from experiments of Hon-nami and Kunito (1998), the concentration of microalgae $C(t)$ in equation (4) is dependent on the growth rate of microalgae (μ_m), which may be described by the logistic function and given below

$$C(t) = C_0 + \frac{a}{1+be^{-\mu_m t}} \quad (5)$$

where, C_0 denotes the suspension's initial concentration a and b are denote the constants.

The following is a one-dimensional energy balance equation: (Androga, Uyar, Koku & Eroglu, 2017)

$$\rho C_p \frac{dT}{dt} = Q_{Total\ radiation} \quad (6)$$

where, $Q_{radiation(total)}$ is the total solar radiation (W) flow from the sun as a function of latitude at every geographical place.

To obtain the radial (r) or axial (z) temperature and concentration gradients, the coupled partial differential equations are as follows (Fogler, 2006)

For the algae cell concentration balance given by the equation

$$D_e \frac{\partial^2 C_i}{\partial r^2} + \frac{D_e}{r}\frac{\partial C_i}{\partial r} + D_e \frac{\partial^2 C_i}{\partial z^2} - U_z \frac{\partial C_i}{\partial z} + r_i = 0 \quad (7)$$

For the Temperature balance given by the equation

$$K_e \frac{\partial^2 T}{\partial z^2} + \frac{K_e}{r}\frac{\partial}{\partial r}\left(r\frac{\partial T}{\partial r}\right) + \Delta H_{Rx} r_A - U_z C_{p_m}\frac{\partial T}{\partial z} = 0 \quad (8)$$

where, D_e represents the effective diffusivity (m^2/s), U_z represents the average velocity in axial direction (m/s), K_e represents the thermal

conductivity (J/m.s.K), C_{p_m} is simply the product of the density of the solution and its heat capacity (J/kg.K)

Boundary and initial conditions

Our simulation treats the microalgae suspension flow as a uniform flow, with zero initial velocity at the inlet, i. e., $\boldsymbol{v} = v_o$; which means there is no slip condition at the reactor's wall and no normal stress at the domain's outlet, which can be represented by

$$[-P\boldsymbol{I} + \eta(\mathrm{t})(\nabla \boldsymbol{v} + (\nabla \boldsymbol{v})^T)].\boldsymbol{n} = 0$$

where, $\boldsymbol{P}$ stands for pressure, and $\boldsymbol{I}$ stands for identity matrix.

For the algae cell concentration and energy balance the boundary and initial conditions for the system are

Initial conditions: If not in a steady state, the initial conditions

$$t = 0, \qquad T = T_0, \qquad C_i = 0, \qquad for\ z > 0\ all\ r$$

Boundary conditions

Radial: We have got symmetry,

$$\frac{\partial C_i}{\partial r} = 0 \quad and \quad \frac{\partial T}{\partial r} = 0 \qquad at\ r = 0$$

On the reaction side, the temperature flux to the wall equals the convective flux out of the reactor into the heat exchanger shell

$$-K_e \frac{\partial T}{\partial r}|_R = U_{ht}\big(T(R,\ z) - T_a\big) \qquad at\ r = R$$

At the tube walls there is no mass flow exists

$$\frac{\partial C_i}{\partial r} = 0 \qquad at\ r = R$$

Axial: At the inlet to the reactor

$$T = T_0 \quad and \quad C_i = C_{i0}\,, \qquad at\ z = 0$$

At the outlet to the reactor

$$\frac{\partial C_i}{\partial z} = 0 \quad and \quad \frac{\partial T}{\partial z} = 0 \qquad at\ z = L$$

Computational domain and mesh design

The computational domain of the horizontal loop tubular photobioreactor (HLTP) with a U-loop, where the straight portion measures 10 meters in length but the U-loop measures approximately 0.5 meters in length. The radius of the reactor is 0.025 meters, it has a surface area of 3.136 meters squared, and its volume is 0.03679 meters cubic, which is shown in Figure 1.

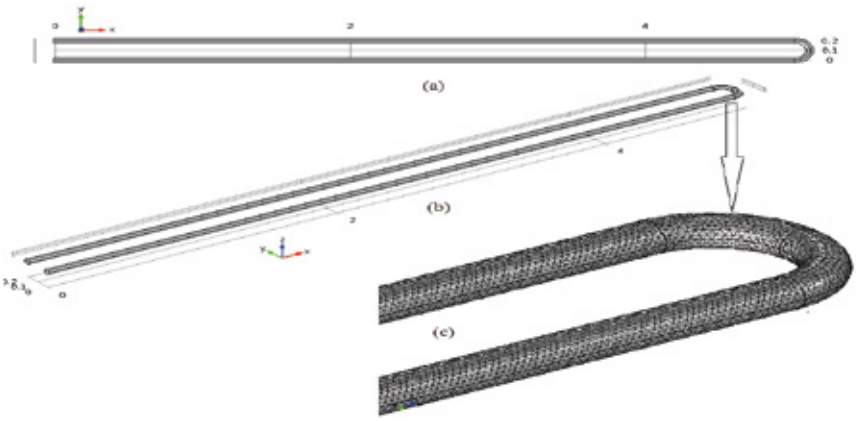

Figure 1
A computational domain of the horizontal loop tubular photobioreactor (HLTP) showing with U-loop mesh.

Simulation parameters

In order to simulate, the simulation's parameters were particularly chosen for the definite region Chittagong University of Engineering & Technology (CUET) in Chittagong, Bangladesh. We have taken into account the *Chlorella* species strain for the broth medium. Table I provides the simulation parameters.

Table I
Parameters which used in our simulation

Symbol	Value	Meaning
R	0.025 m	Reactor's radius
V	0.03679 m^3	Reactor's volume
A	3.136 m^2	Reactor's area
IR_{air}	1	Air's coefficient of refraction
IR_{tube}	1.49	Acrylic tube's refraction coefficient
ϕ	22.46^0	Latitude at CUET
N	75	The calendar day on which the simulation is performed
ε	0.94	Reactor's emissivity
K_a	36.9 m^{-1}	The probability of *Chlorella vulgaris* extinction
μ_{max}	0.0631 h^{-1}	Maximum rate of microalgae growth
a	1	Value of the constant
b	200	Value of the constant
C_0	0.55 g/L	Microalgae's primary concentration
μ_0	0.001 Pa.s	Viscosity of water
G_{on}	1367 W/m^2	The constant of the sun
PL	0.03 m	Radiation's path length
K_d	0.33	Diffused reaction's fraction
S	8.1 h	In march, bright sunlight hour

Results with discussions

The objective of this simulation is to analyze the radial and axial temperature variations within the photobioreactor and their corresponding impact on the growth of microalgae. This investigation is limited to a particular geometry, species, and location. All relevant parameters have been taken into consideration for the outdoor cultural conditions. It is assumed that the photobioreactor will receive varying intensities of solar radiation throughout the day, ranging from morning to evening.

Axial temperature profiles

Figure 2.1 to Figure 2.3 demonstrate the axial temperature profiles at various vertical cross-sectional positions of the domain at the same time 11:50 AM. We found that the temperature varies from 294K to 302K at different positions of the reactor geometry and does not follow any common profile.

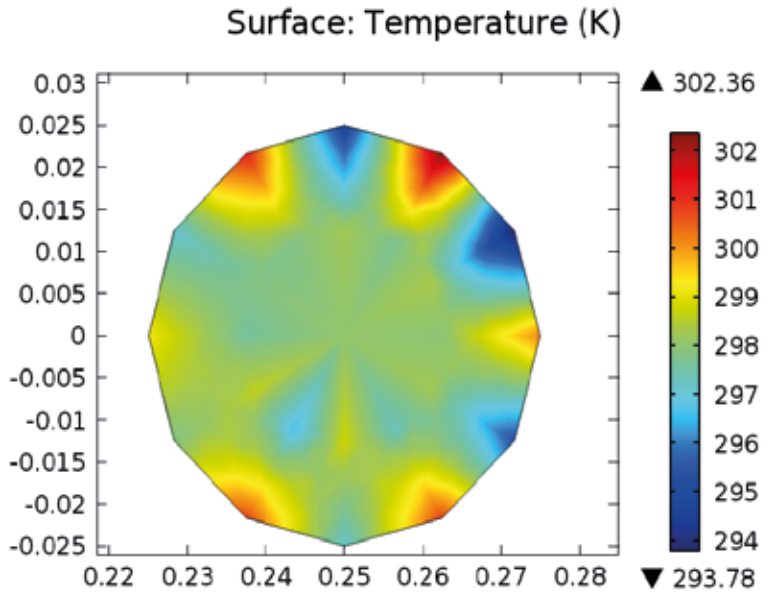

Figure 2.1

Axial temperature profiles on the vertical cross-section taken at 11:50 AM, when $x = 2m$ *(measured from outlet).*

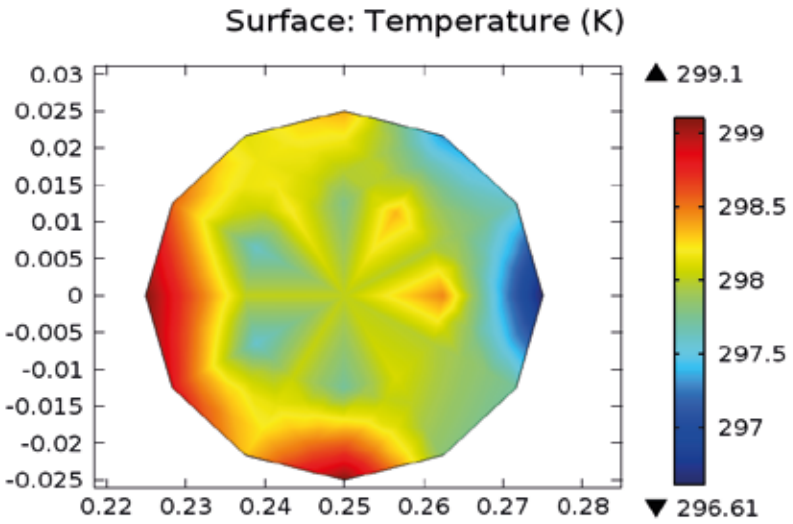

Figure 2.2

Axial temperature profiles on the vertical cross-section taken at 11:50 AM, when $x = 4m$ *(measured from outlet).*

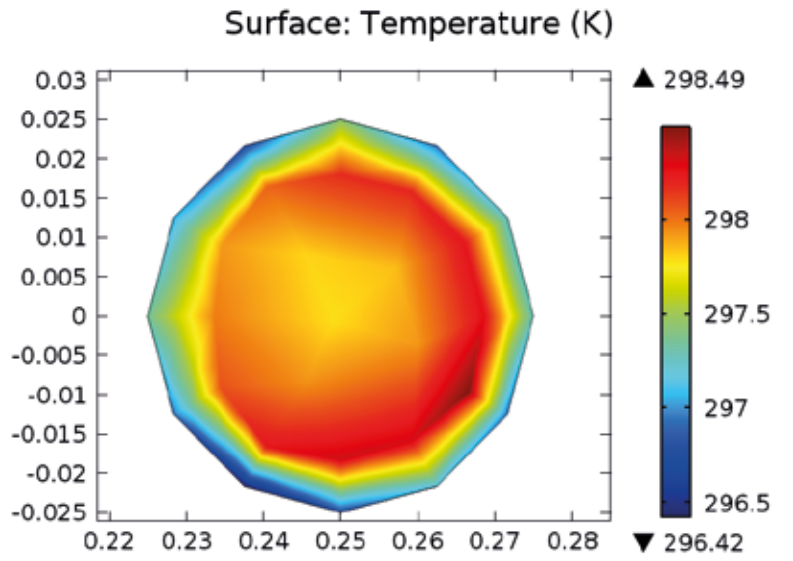

Figure 2.3

Axial temperature profiles on the vertical cross-section taken at 11:50 AM, when $x = 8m$ *(measured from outlet).*

Figure 2.4 shows the overall line graph of the axial temperature magnitudes at the different position of vertical cross-sections of the domain at the same time 11:50 AM and Figure 2.5 shows the overall line graph of axial temperature magnitudes of different times between 8:50 AM to 11:50 AM. It shows that the variation of temperature is not significant. However, the temperature is a bit higher in the middle compared to the wall.

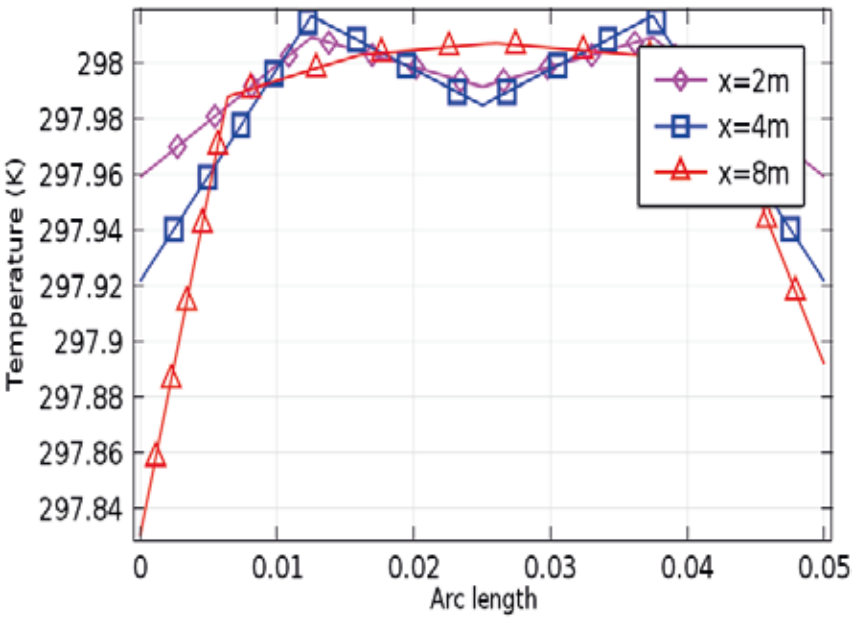

Figure 2.4
Overall line graphs of the axial temperature magnitudes on the vertical cross-section taken at 11:50 AM when, $x = 2, x = 4$ *and* $x = 8$ *(measured from outlet).*

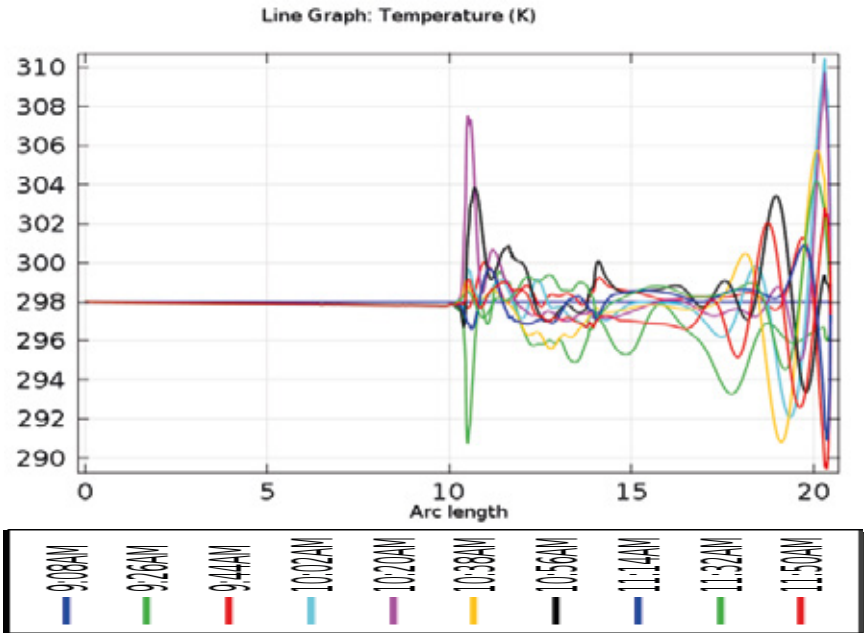

Figure 2.5
Overall line graphs of the axial temperature magnitudes of different times between 8:50 AM to 11:50 AM.

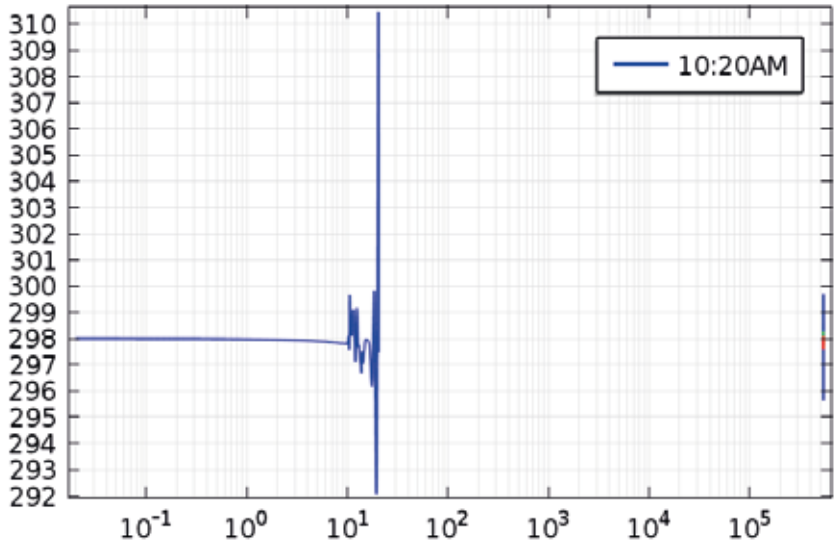

Figure 2.6
The line graph of the axial temperature magnitudes at 10:20 AM.

From the axial temperature profiles shown in the above Figure 2.1 to Figure 2.3, it is noticed that at the same time 11:50 AM the temperature is gradually decrease while distance is increasing from the outlet of the tubular reactor. As a result, the temperature will be at its highest near the reactor's outlet, as shown by the overall line graphs of the axial temperature magnitudes by the Figure 2.4. Figure 2.5 show the axial temperature variations along the axial length at various times. The figures show that the axial temperature fluctuates from the U-loop's intake to its outlet while remaining the same for the inlet to the U-loop. The reason behind this is that while the culture crosses the U-loop, a little turbulent is created which is observed from the velocity profile. Hence, the dark part of the culture comes to the wall side and vice versa which results axial temperature variations after the U-loop. Before U-loop the culture flow was almost laminar where axial temperature remains constant. Also the maximum axial temperature was found about 312K at 10:20 AM near the outlet of the tubular reactors, which is shown in Figure 2.6.

Radial temperature profiles

Figure 2.7 to Figure 2.9 show the line graph of the magnitudes of radial temperature on the vertical cross-sections at outlet of the domain at the different times and Figure 2.10 shows the overall line graph of the radial temperature magnitudes at outlet at the different times. On the other hand, Figure 2.11 and Figure 2.12 show the minimum radial temperature profiles at the time 9:08 AM and the maximum radial temperature profiles at the time 10:20 AM of the tube respectively. Finally, Figure 2.13 shows the overall line graph of the radial temperature magnitudes between the times 8:50 AM to 11:50 AM.

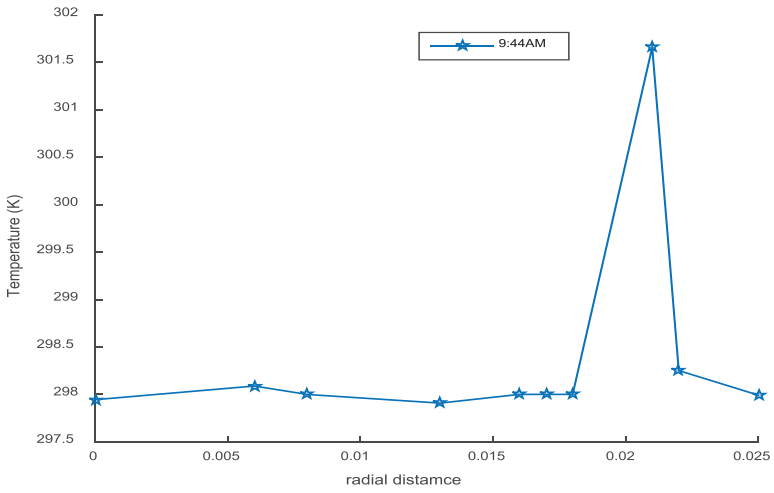

Figure 2.7
The line graph of the radial temperature magnitudes at outlet on vertical cross section at 9:44 AM.

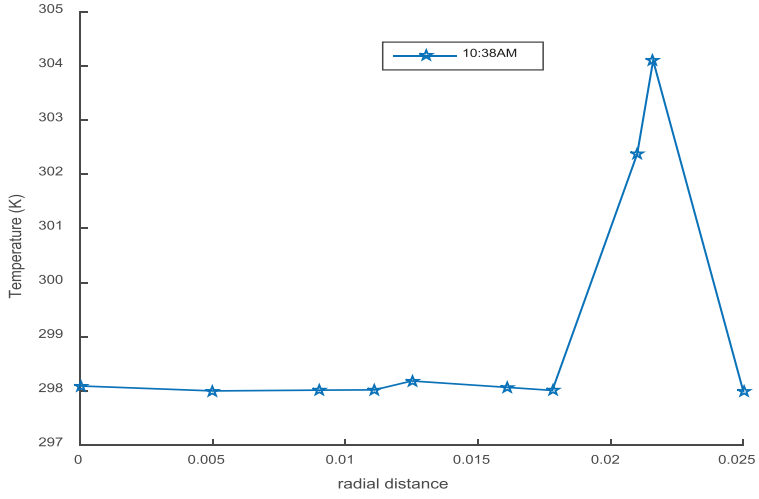

Figure 2.8
The line graph of the radial temperature magnitudes at outlet on vertical cross section at 10:38 AM.

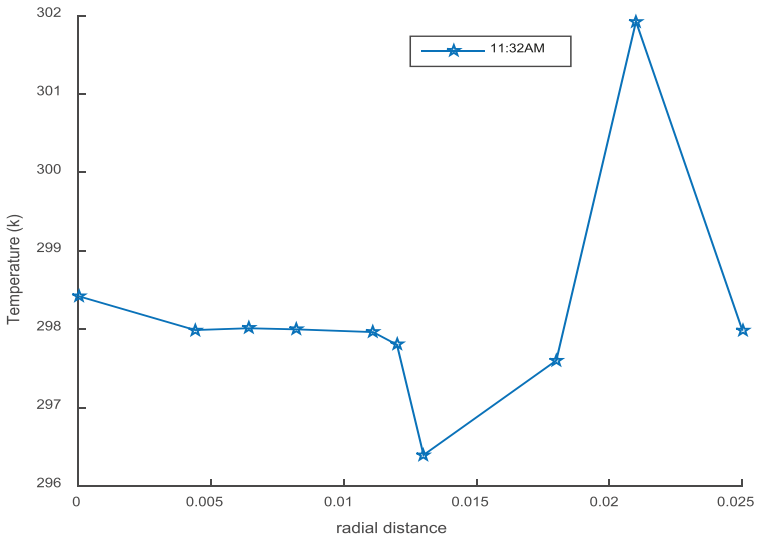

Figure 2.9
The line graph of the radial temperature magnitudes at outlet on vertical cross-section at 10:38 AM.

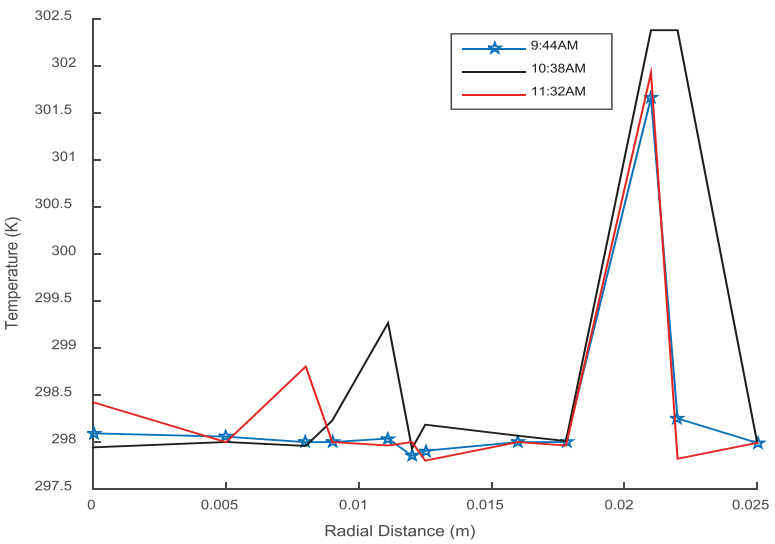

Figure 2.10
Overall line graph of the radial temperature magnitudes at outlet at the different time 9:44 AM, 10:38 AM and 11:32 AM respectively.

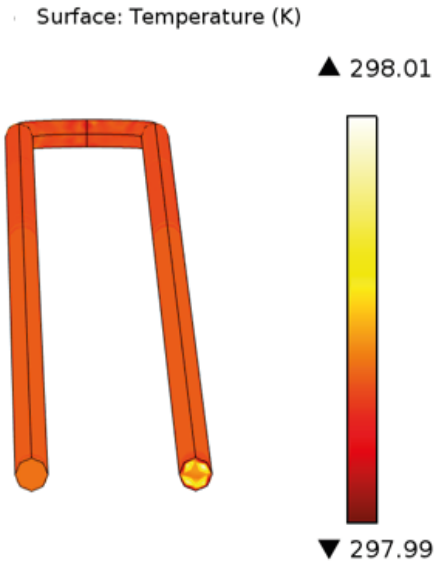

Figure 2.11
Overall radial temperature profiles at the time 9:08 AM.

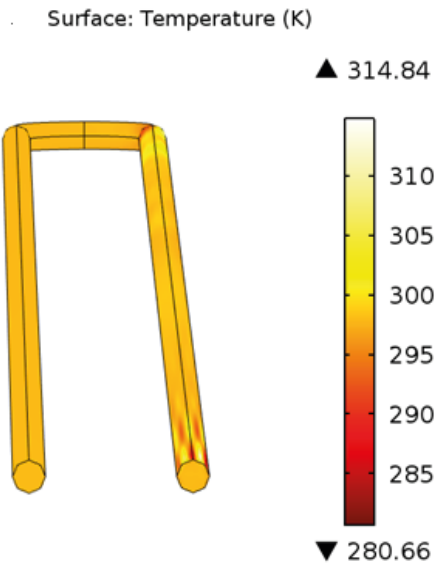

Figure 2.12
Overall radial temperature profiles at 10:20 AM.

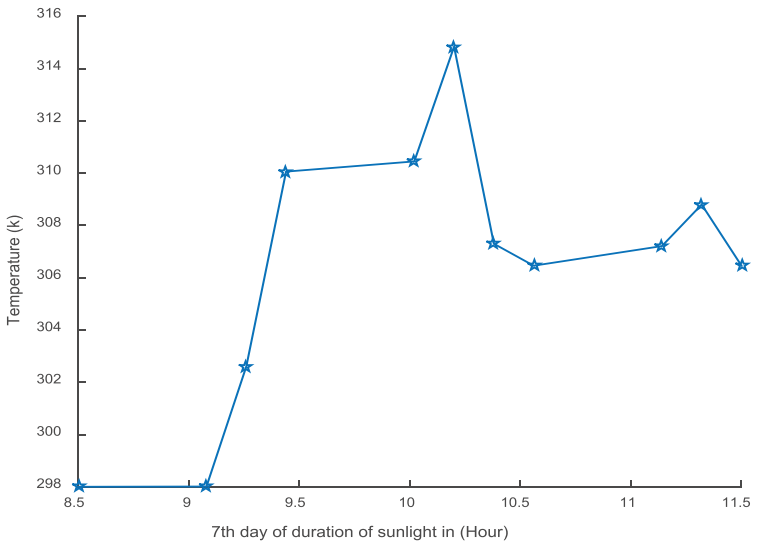

Figure 2.13
Overall the line graph of the radial temperature magnitudes at outlet between the times 8:50 AM to 11:50 AM.

From the line graphs of the radial temperature profiles shown in the above figures, we observed that the minimum temperature is at center of the radial cross section of the domain and it is continuously fluctuates through the line along center to upper circumference. It is also noticed that the radial temperature fluctuations are almost same with respect to time variations which are shown by the figure 2.10. Most of the time, the temperature was found to be higher near the reactor wall than in the middle of the tube for the radial part. Along the radial axis the minimum temperature shows near 298K at 9:08 AM and the maximum temperature noted near 314K at 10:20 AM which are shown by the figure 2.11 and figure 2.12 respectively.

Conclusion

The axial and radial temperature variations for HLTP at different positions are simulated in this study. A computational model based on temperature effect is considered to simulate this result. We analyzed that the temperature variation is insignificant for the axial part of the tubular reactor from the inlet to the start of the U-loop. However, a marginal variation is observed for the U-loop and rest of the part of the reactor domain. Most of the time, the temperature was found to be higher on the

wall than in the middle of the tubular reactor for the radial part. It is noted that a maximum temperature is near 312K through the axial direction and a maximum temperature is near 314K through the radial direction of the culture which was beyond the optimal temperature range 293K - 308K.

Acknowledgements

The author gratefully acknowledges the Center of Excellence in Mathematics, Department of Mathematics at Mahidol University in Bangkok 10400, Thailand and the Simulation Lab of the Department of Mathematics at the Chittagong University of Engineering & Technology, both of which provided technical supports.

References

Androga, D., Uyar, B., Koku, H., & Eroglu, I. (2017). Dynamic modeling of temperature changes in outdoor operated tubular photobioreactors. *Bioprocess and Biosystems Engineering, 40*(7), 1017-1031. doi: 10.1007/s00449-017-1765-3

Chang, J. S., Show, P. L., Ling, T. C., Chen, C. Y., Ho, S. H., Tan, … Pandey, A., (2017). Photo-Bioreactors, *Current Developments in Biotechnology and Bioengineering: Bioprocesses, Bioreactors and Controls,* Elsevier, Atlanta, 313-352. https://doi.org/10.1016/B978-0-444-63663-8.00011-2

Chisty Y. (2007). Biodiesel from microalgae, *Biotechnology Advances,* vol. 25, 294-306. https://doi.org/10.1016/j.biotechadv.2007.02.001

Deb, U. K., Shahriar, M., Bhowmik, J., & Chowdury, M. K. H. (2017). The effect of irradiance related temperature on microalgae growth in a tubular photo bioreactor for cleaner energy. *American Journal of Computational Mathematics, 7*, 371-384. https://doi.org/10.4236/ajcm.2017.73026

Einstein, A. (1906). Eine neue Bestimmung der Moleküldimensionen. *Ann. de. phys., 19*, 289-306

Fogler, H. S. (2006). *Elements of Chemical Reaction Engineering*, Fourth dition

Hon-nami, K., & Kunito, S. (1998), Microalgae cultivation in a tubular bioreactor and utilization of their cells. *Chinese Journal of Oceanology and Limnology, 16*(S1), 75-83. doi: 10.1007/bf02849084

Khanam, I. A., & Deb, U. K. (2016). Calculation of the average irradiance and the microalgae growth for a year at CUET, Bangladesh. *American Journal of Computational Mathematics, 6*, 237-244. http://dx.doi.org/10.4236/ajcm.2016.63024

Smith, V. H., Sturm, B. S. M., Noyelles, F. J., & Billings, S. A. (2010). The Ecology of Algal Biodiesel Production. *Trends in Ecology & Evolution*

(Personal Edition), 25, 301-309. http://dx.doi.org/10.1016/j.tree.2009.11.007

Su, Y., Song, K., Zhang, P., Su, Y., Cheng, J., & Chen, X. (2017). Progress of Microalgae Biofuel's Commercialization. *Renewable and Sustainable Energy Reviews,* 74, 402-411. https://doi.org/10.1016/j.rser.2016.12.078

Tredici, M. R. (1999). Photo Bioreactors *In Encyclopedia of bioprocess technology: fermentation, biocatalysis and bioseparation,* edited by Flickinger MC, Drew SW (Wiley & Sons) USA. pp. 395–41